Heat treatment induced martensitic accommodation and adaptive anisotropy in melt spun Ni55Mn22Ga23 (at. %) ribbons

Satnam Singh, R. K. Roy, M. Ghosh, A. Mitra, and A. K. Panda

Citation: J. Appl. Phys. **112**, 103512 (2012); doi: 10.1063/1.4765739
View online: http://dx.doi.org/10.1063/1.4765739
View Table of Contents: http://jap.aip.org/resource/1/JAPIAU/v112/i10
Published by the American Institute of Physics.

Heat treatment induced martensitic accommodation and adaptive anisotropy in melt spun $Ni_{55}Mn_{22}Ga_{23}$ (at. %) ribbons

Satnam Singh, R. K. Roy, M. Ghosh, A. Mitra, and A. K. Panda[a)]
CSIR-National Metallurgical Laboratory, Jamshedpur 831007, India

(Received 30 November 2011; accepted 17 October 2012; published online 21 November 2012)

The effect of annealing on melt spun $Ni_{55}Mn_{22}Ga_{23}$ (at. %) ribbon has been addressed in terms of structural, thermal, thermomagnetic, and magnetic field induced strain (MFIS) behaviour. In comparison to as-spun ribbons, the samples annealed within the $L2_1$ domain at 1073 K for 30 h with subsequent furnace cooling, showed a rise in martensitic transformation temperature. This was endorsed from electron microscopy studies revealing change in morphology of martensite plate and stacking of dislocations in a preferential orientation. The mechanism is associated to martensitic accommodation which enhanced ferro-elastic magnetic coupling and also lowered magnetic coercivity. Such accommodations and adaptive anisotropy improved the MFIS behavior in the annealed sample. © *2012 American Institute of Physics*. [http://dx.doi.org/10.1063/1.4765739]

I. INTRODUCTION

Martensitic transformation and magnetic transition (Curie temperature) characteristics are important signatures for generating magnetic field induced strains (MFIS) in ferromagnetic shape memory alloys (FSMAs). The traversal path A2 → B2′ → $L2_1$ → M circumscribes a range of order-disorder phenomena. The transformation route is catalysed by elemental migrations as well as evolution of stress induced martensites (SIMs). In the NiMnGa system, the element Ga diffuses much slower than the other elements. Therefore, Ni and Mn strongly affect order-disorder transformations.[1] Similarly, during B2′ → $L2_1$ transformation, the disorder between elements Mn and Ga plays a key role towards ordering mechanism.[2] In this case, $L2_1$ is a highly ordered[3] phase. However, the degree of ordering is highest when quenched from 1073 K.[4]

Quenching and heat treatment are part of the intrinsic thermo-mechanical and thermo-magnetic procedures wherein phenomena like grain boundary diffusion, twinning of martensite, and stress relaxation occur in nano-micro regime. Such thermal treatments induce desired equilibrium phases in the parent phase. Generation of such phases is far more controlled when proceeding from a rapid solidification process like melt spinning wherein the sheet type actuator can be directly produced in a single step process. In recent years, Heusler structure in FSMAs has also been recently obtained by rapid quenching techniques like melt-spinning[5,6] with a potentiality of impeding undesirable γ-phase[7] that is detrimental towards shape memory effect. In rapid solidification route, the high temperature frozen-in-structure bears unaccommodated and stressed martensite as well as the parent phase. Thus, the quenching temperature (QT) is critically important to modify long range ordered (LRO) structure. It is known that as QT increases, LRO decreases along with a reduction in onsets of structural (martensitic) and magnetic (Curie) transformation.[8,9] Therefore, to induce reversal in the phenomenon of quenched structure, the controlled heat-treatment is a way to enhance martensitic structure and its scope of accommodation through normal cooling. It is particularly important in context of the fact that magnetic field driven shape deformation will be high with greater magneto-crystalline anisotropy of martensite.[10] Consequently, on application of an uniaxial magnetic field in a multivariant system, the growth of some martensitic variants will increase the magnetocrystalline anisotropy energy.[11,12] The high energy of magnetic anisotropy, configuration/orientation of dislocations, and density of twinned martensitic plates are expected to play a pivotal role in enhancing the MFIS in ferromagnetic shape memory systems.[13–15]

The present work is focused on the effect of annealing on the melt spun ribbons of a NiMnGa alloy. The structural, magnetic, and magneto-strain behaviors of annealed ribbon samples have been investigated with respect to their as-spun ones. The correlation throws light on the martensitic features post heat-treatment and the consequent effect on different properties of the investigated FSMA.

II. EXPERIMENTAL

The $Ni_{55}Mn_{22}Ga_{23}$ (at. %) alloy was prepared using an arc melting furnace in argon atmosphere and then melt-spun into ribbons using a melt spinner with a quenching wheel made of copper rotating with its peripheral velocity of 23 m/s. Ingots and ribbons were sealed in quartz ampoules and annealed at 1073 K for 30 h and subsequently furnace cooled. The phases in as-prepared ingot (#I_{SN}), annealed ingot (#I_{AN}), as-spun (#R_{SN}), and annealed (#R_{AN}) ribbons were identified at room temperature using Bruker AXS D8 x-ray diffractometer with Cu-Kα radiations operating at scan rate of one degree per minute. The microstructures were observed using a transmission electron microscope (TEM; Philips CM200). The room temperature magnetization was carried out at a rate of 0.005 T/s while thermomagnetic plots were obtained at 2 K/min using vibrating sample magnetometer (LakeShore, VSM-7404). Phase transformation

[a)]Author to whom correspondence should be addressed. Electronic addresses: akpanda@nmlindia.org and akpanda2_in@rediffmail.com. Tel.: +91 657 2345002. Fax: +91 657 2345213.

temperatures were measured at a scan rate of 15 K/min using a differential scanning calorimeter (Perkin Elmer, Diamond DSC). The MFIS in the ribbons was determined using a measurement system involving a device based on capacitive technique developed in the laboratory. In this device, the ribbon sample is placed between parallel plate capacitors. With the application of field, the dimensional change leads to a change in capacitance which was measured and strain generated in parts per million (ppm) was calculated.

III. RESULTS AND DISCUSSION

Microstructural studies on as-spun and annealed ribbons were carried out, wherein TEM bright field images were obtained. The as-spun ribbon exhibited martensite phase with plate morphology and plate thickness in the range of 5–15 nm as shown in Fig. 1(a). Within prior austenite grain, the orientation of the cluster remained same and likely to be parallel to the parent phase habit plane. The existence of dislocation network indicated (Fig. 1(b)) lattice strain associated with shear transformation. The interplanar spacing between successive plates was within a narrow range of 25–35 nm. The martensitic plates in the as-spun ribbons indicated a high density of dislocations in a regular fashion as shown in Fig. 1(b). These appear as wavy stacking fault fringes[16] which are very closely placed along the plate length. An interesting effect of annealing at 1073 K/30 h was observed on martensite morphology (Fig. 2). Annealing enhanced the grain boundary migration of martensite plates in the matrix. As a result, thinner plates were eaten up by relatively larger ones leading to an increase in plates width ~70–80 nm. The successive plates ran parallel to each other and were equally spaced. The annealing also enhanced the mobility of dislocations as showed in Figs. 2(a) and 2(b). The well known polygonisation was observed in the form of "dislocation pile-ups" near twin boundaries (white circles, Fig. 2). The strain was automatically reduced by the annihilation of defects during annealing. The dislocation orientations after annealing have taken the path along the plate length in a direction parallel to the plane (220) as shown in the selected area diffraction (SAD) pattern (inset of Fig. 2(b)). Thus, the propagation of dislocations has also taken place along the martensite plates during the thermally induced twinning and de-twinning process occurring while heating and cooling cycle, respectively.

The transformation of a low symmetric structure (martensitic) to a highly symmetric one (austenitic) and vice-versa is induced by absorption or evolution of the heat,

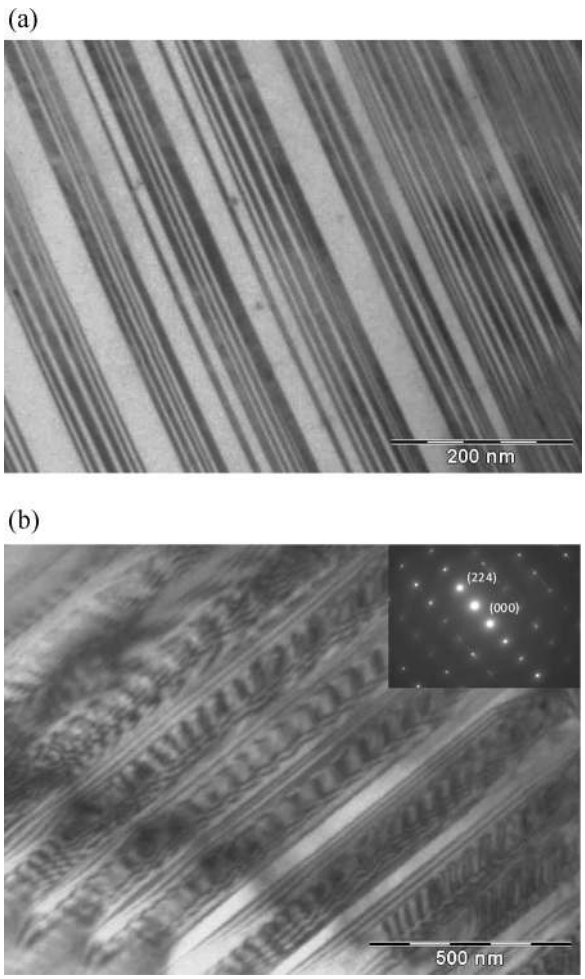

FIG. 1. TEM microgarphs of (a) martensitic plate morphology and (b) dislocation pattern in as-spun ribbons. SAD in the inset of "b" indicated plate orientation.

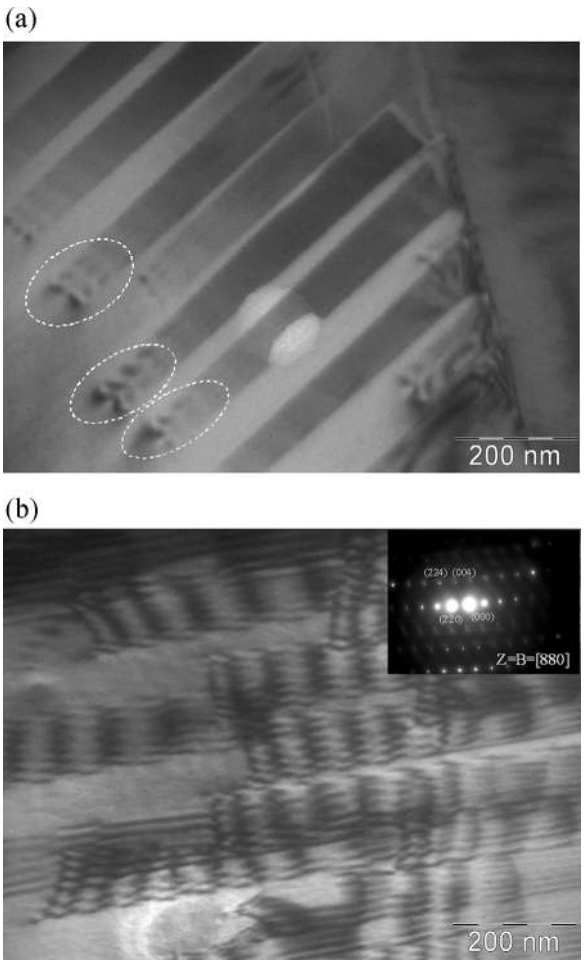

FIG. 2. TEM microgarphs of (a) martensitic plate morphology with dislocation pile-ups (white circles) and (b) dislocation pattern in ribbons at 1073 K for 30 h. SAD in the inset of "b" indicated plate orientation.

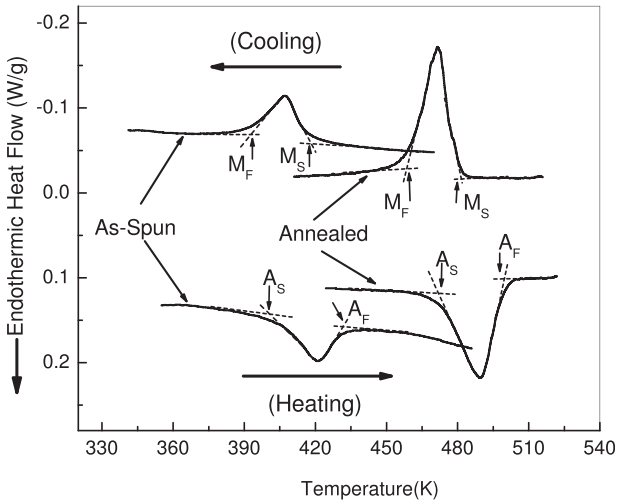

FIG. 3. DSC plots of as-spun and annealed ribbons.

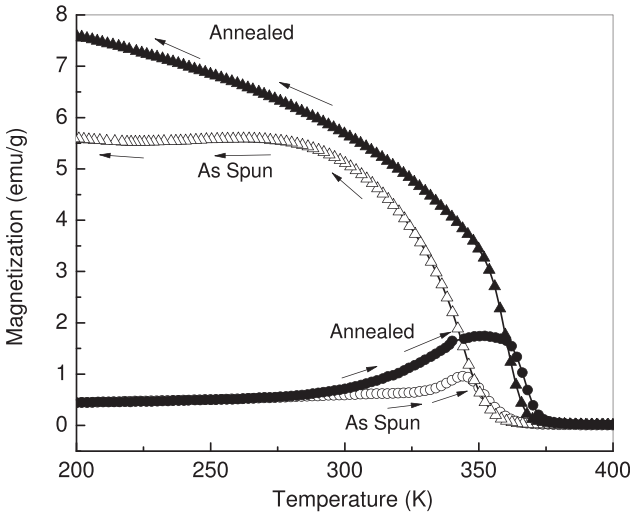

FIG. 4. Thermomagnetic plots of as-spun and annealed ribbons.

respectively, by the system. The DSC heat flow profiles (Fig. 3) of as-spun ($\#R_{SN}$) and annealed ribbons ($\#R_{AN}$) revealed endothermic and exothermic peaks during heating and cooling cycle. It was interesting to note that as-spun sample manifested a shift in the transformation towards elevated temperature when annealed at 1073 K for 30 h. The DSC characteristic temperatures obtained from thermal cycles are shown in Table I. It was observed that after the annealing treatment, the increase in the martensitic (ΔM_S) and austenitic (ΔA_S) transformation onsets was 62 K and 63 K, respectively. This suggests an enhanced diffusion less mechanism playing role at an elevated temperature of 1073 K that was below $L2_1 \leftrightarrow B2'$ transformation interphase reported to be at 1173 K.[17] It is expected that the chemical ordering during 30 h of soaking period had occurred in view of a low ordering time of 0.1 s for Mn in Ni to 35 s for Ni in Ni even at a lower temperature of 873 K. This span of ordering suggests that the accommodation and martensitic reordering phenomenon occur when the material is furnace cooled from 1073 K to a temperature below M_S. In the annealed samples, the enhancement in volume fraction of martensitic is also evidenced from enthalpy data. It is also observed that the enthalpy of martensitic transformation and its reverse for the annealed sample is 7.70 J/g and 7.90 J/g, which is almost twice that of as-spun ribbon with values of 3.8 J/g and 4.10 J/g, respectively.

Considering the ratio M_S/T_m as an indicator to determine the diffusion velocity, the values have been found to be 0.30 and 0.34 for as-spun and annealed ribbons, respectively, wherein M_S is the martensitic start temperature and $T_m \sim 1400$ K is the melting point for a typical $Ni_{54}Mn_{25}Ga_{21}$ alloy.[18] The high values of diffusion velocity contributed to rise in austenitic start (ΔA_S) ~ 62 K and martensitic start (ΔM_S) ~ 63 K (Table I) after annealing. This rise is attributed to the rearrangement of atoms and suitable accommodation within martensitic sites. This accommodation and enhanced ordering led to increase in the Curie temperature after annealing as observed from thermo-magnetic cycles (Fig. 4). The rise in Curie temperature was $\sim$14–16 K in annealed sample. The small hysteresis of 8 K and 6 K during thermal cycles for as-spun and annealed samples, respectively, may be due to thermal lag in the measurement system.

The modification in the ordering mechanism with annealing has been found to affect the magnetic properties and MFIS. Upon annealing, the saturation magnetization "σ_S" increased from as-spun values of 40 emu/g to 47 emu/g as shown in Fig. 5(a). Similarly, the coercivity values decreased from 26 mT are as-spun state to 7 mT in annealed sample (inset of Fig. 5(a)). The rise in magnetization is attributed to increase in flux density in the broadened martensite plates and also due to changes in austenite phase. Moreover, the ferroelastic domain coupling on these stress-induced maturing martensites needs lower magnetization energy leading to lowered coercivity in annealed state. From the initial magnetization plots, the effective anisotropy constant K_{eff} is calculated using mathematical expression

$$K_{eff} = 1/2 \int_0^{\sigma_S} H.dM, \tag{1}$$

TABLE I. Characteristic temperatures and enthalpies obtained from DSC and thermomagnetic studies of as-spun and annealed ribbons. A_S, austenitic start; A_f, austenitic finish; M_S, martensitic start; M_f, martensitic finish; ΔH_H, enthalpy heating; ΔH_C, enthalpy cooling; T_{CH} and T_{CC}, Curie temperature heating and cooling cycles, respectively.

	A_S (K)	A_f (K)	ΔH_H (J/g)	T_{CH} (K)	M_S (K)	M_f (K)	ΔH_C (J/g)	T_{CC} (K)
As-Spun (# SN)	409	432	4.10	352	415	392	3.8	344
Annealed (# AN)	472	498	7.90	366	477	461	7.70	360
Post-annealing change, Δ	63	66	3.80	14	62	69	3.90	16

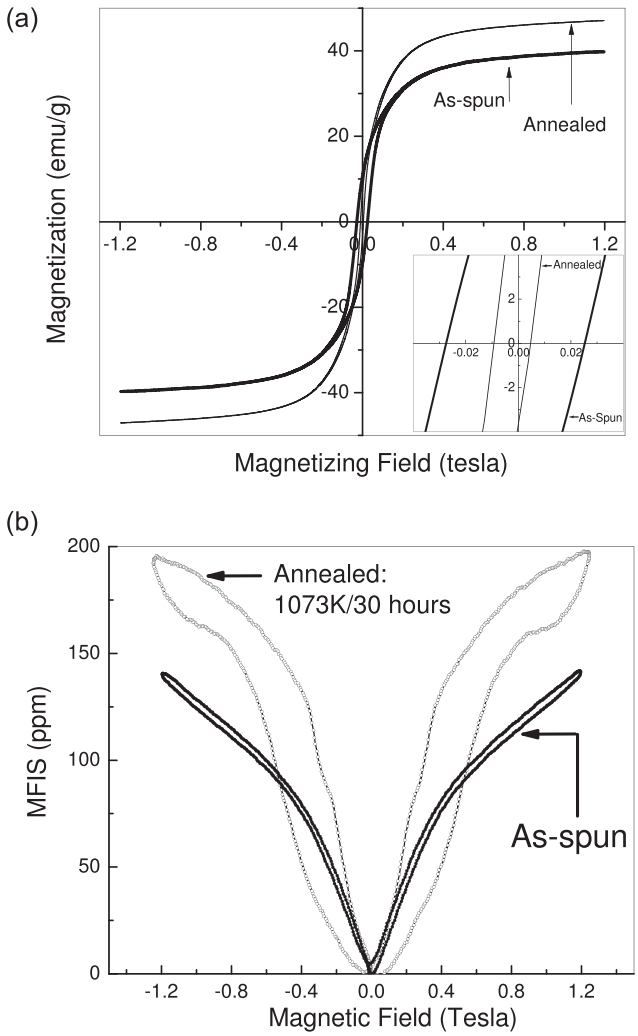

FIG. 5. (a) Magnetization plots and (b) MFIS of as-spun and annealed ribbons.

where H is the applied field and M stands for magnetization. At the applied maximum field of 1.2 T, the annealed sample had K_{eff} of 3.19 J/kg which was higher than that of 3.05 J/kg for as-spun ribbon. The enhanced K_{eff} is attributed to enhanced martensite volume fraction and accommodation in preferred orientation. The martensitic phase raises the K_{eff} as it does in case of stoichiometric Ni_2MnGa.[19] The as-spun and annealed ribbon samples displayed interesting MFIS behavior. The as-spun ribbon revealed a MFIS value of 141 ppm at an applied field of 1.19 T as shown in Fig. 5(b). However, the strain value of annealed sample reached as high as 196 ppm, regarding to the enhanced martensitic state. It makes the sample capable enough to accommodate higher strain variations with magnetizing field. The MFIS cycle showed broader hysteresis in annealed sample. This is associated to twinning and de-twinning mechanisms in these broad martensite plates. It was also observed that the strain variation was relatively high below 0.4 T which was also evidenced from the magnetization behavior (Fig. 5(a)), wherein the drastic variation in induction below this field suggests rapid magnetic domain movements that are ferro-elastically coupled to the martensitic twin variants.

The rearrangement and accommodation mechanism of martensitic phase after cooling down from an elevated annealing temperature of 1073 K were also reflected in the lattice reflections as observed from the x-ray diffractograms (Fig. 6(a)). The diffractograms indicate an enhanced intensity of the martensitic primary phase (M_{112}) and higher order reflections (M_{200}, M_{004}, M_{220}, M_{204}, M_{312}, M_{224}) with an additional and prominence of M_{116} peak in the ribbon samples annealed at 1073 K. The austenite peak A_{220} has been found to be present even after annealing at elevated temperatures of 1073 K and 1273 K. The presence of a fraction of B2 phase along with $L2_1$ austenite phase is not completely ruled out presently. This is also supported by the remnant B2 observed during rapid quenching.[20,21] The synergistic reduction in austenite phase which contributes to increase in saturation magnetization as well as enthalpy with annealing temperature needs further investigation.

To further elucidate the effect of annealing on melt spun ribbon, the ratio of ($\#R_{AN}/\#R_{SN}$) martensitic phase reflection intensities of annealed ribbon with respect to as-spun ribbon sample is shown in Fig. 7. In the case of ribbon sample, it is observed that M_{220} peak intensities indicated significant evolution of martensitic phase in ribbon after annealing at 1073 K for 30 h. Such evolution post annealing was evident from splitting of peak M_{112} in samples annealed for 30 h at 1073 K and also at 1273 K (inset Fig. 7). This splitting may be attributed to growth of 2 M modulation in tetragonal martensite phase during annealing. It is also understood that the habit plane pertaining to parent phase A_{220} facilitates martensite evolution with a distinct enhancement in M_{220} peak intensity. The prominence of diffraction spot (220) in annealed sample (inset of Fig. 2(b)) compliments the above observation. The strong anisotropic texture along this plane is also expected in post annealing treatment. The other martensitic orientations have been found to be accommodative with distinct signatures of increasing intensity after annealing. However, the intensity ratios of as-prepared ingot with respect to its annealed state given by ($\#I_{AN}/\#I_{SN}$) did not indicate significant enhancement in martensitic phase which was observed in the case of ribbon samples.

Structural and magnetic evaluations showed that post annealing treatment induced a distinct advantage of melt spinning in consequent martensitic accommodation and the adaptive anisotropy in melt spun ribbons. This also has been found to influence the lattice strain[22,23] given by

$$\varepsilon_{\text{lattice}} = \beta/(4\tan\theta) + \lambda/\text{d}, \tag{2}$$

where β is experimentally observed full width half maxima (FWHM) of peak, λ is the wavelength, d is grain size, and θ is the diffracting angle. In view of the large grain size $\sim$microns, the contribution of second term has been neglected. From this relation, $\varepsilon_{\text{lattice}}$ was found to be 6.39×10^{-3} in as-spun ribbons and it was reduced to 5.45×10^{-3} after annealing. Such reduction cannot be accredited only towards stress relaxation but also due to suitable martensitic accommodation. After annealing at 1073 K for 30 h, the volume fraction of martensite increases as evidenced from reflection intensities (Fig. 6(a)). The dominance

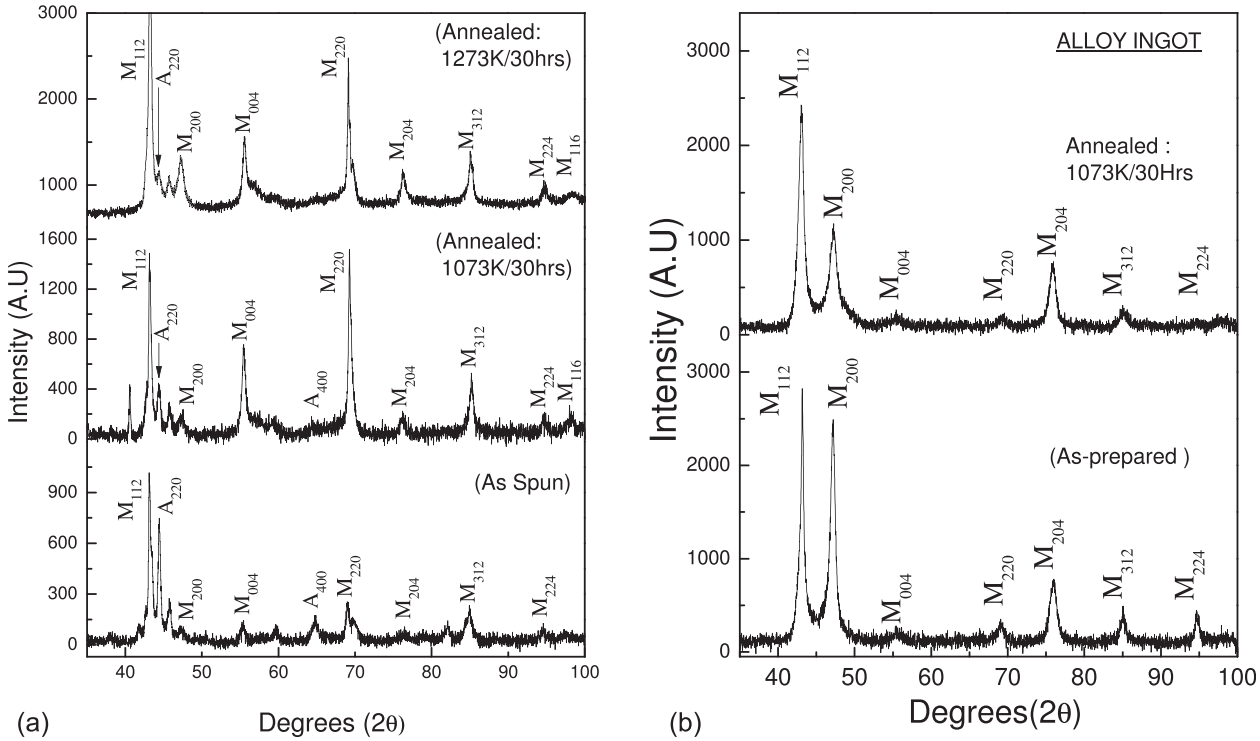

FIG. 6. X-ray diffraction patterns of (a) ribbon and (b) alloy ingot in as-prepared and annealed states.

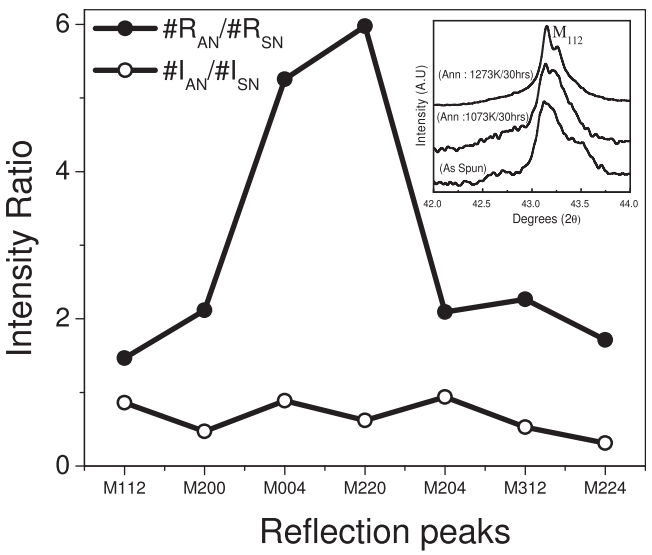

FIG. 7. Variation of martensite peak intensities ratios in ribbon ($\#R_{AN}/\#R_{SN}$) and ingot ($\#I_{AN}/\#I_{SN}$). Inset showing splitting of M_{112} peak attributed to growth of 2 M modulation.

of this phase reduced the lattice strain between austenite to martensite thereby lowering the net value of $\varepsilon_{lattice}$. This is also attributed to dislocation pile-ups and subsequent annihilation of defects during annealing as observed from microstructural investigation (Fig. 2(b)).

IV. CONCLUSIONS

The effect of annealing on melt spun $Ni_{55}Mn_{22}Ga_{23}$ (at. %) ribbons has been investigated. Compared to the as-spun ribbons, annealing at 1073 K for 30 h, led to an enhancement in martensitic state with a rise in martensitic transformation temperatures (A_S, M_S). The melt spun ribbons revealed advantages of martensite enhancement after annealing treatment. Martensite plate width increased along with dislocation pile-ups suggesting suitable accommodation of plates and adaptive anisotropy. These phenomena increased magnetization, reduced coercivity, as well as improved the MFIS in heat treated ribbons.

ACKNOWLEDGMENTS

The authors express sincere gratitude to Director, National Metallurgical Laboratory, Jamshedpur for kindly giving permission to publish the work.

[1]G. Erdelyi, H. Mehrer, A. W. Imre, T. A. Lograsso, and D. L. Schlagel, Intermetallics **15**, 1078 (2007).
[2]M. Kreissl, K.-U. Neumann, T. Stephans, and K. R. A. Ziebeck, J. Phys. Condens. Matter **15**, 3831 (2003).
[3]P. J. Webster, K. R. A. Ziebeck, S. L. Town, and M. S. Peak, Philos. Mag. B **49**, 295 (1984).
[4]J. Saltys, Acta Phys. Pol. A **47**, 521 (1975).
[5]Z. H. Liu, H. Liu, X. X. Zhang, M. Zhang, X. F. Dai, H. N. Hu, J. L. Chen, and G. H. Wu, Phys. Lett. A **329**, 214 (2004).
[6]A. K. Panda, S. Singh, R. K. Roy, and A. Mitra, J. Magn. Magn. Mater. **323**, 1161 (2011).
[7]Z. H. Liu, M. Zhang, Y. T. Cui, Y. Q. Zhou, W. H. Wang, G. H. Wu, X. X. Zhang, and G. Xiao, Appl. Phys. Lett. **82**, 424 (2003).
[8]V. Sanchez Alarcos, V. Recarte, J. I. Perez-landazabal, and G. I. Cuello, Acta Mater. **55**, 3883 (2007).
[9]T. Goryczka, M. Gigla, and M. Morawiec, Int. J. Appl. Electromagn. Mech. **23**, 81 (2006).
[10]K. Ullakko, J. K. Huang, C. Kantner, R. C. O'Handley, and V. V. Kokorin, Appl. Phys. Lett. **69**, 1966 (1996).
[11]T. Fukuda, T. Sakamoto, T. Kakeshita, T. Takeuchi, and K. Kishio, Mater. Trans. **45**, 188 (2004).
[12]Y. Murakami, D. Shindo, K. Kobayashi, K. Oikawa, R. Kainuma, and K. Ishida, Mater. Sci. Eng., A **438**, 1050 (2006).

[13]A. A. Likhachev and K. Ullakko, Phys. Lett. A **275**, 142 (2000).
[14]A. A. Likhachev and K. Ullakko, J. Phys. IV **11**, 293 (2001).
[15]A. Sozinov, A. A. Likhachev, and K. Ullakko, IEEE Trans. Magn. **38**, 2814 (2002).
[16]Y. Ge, N. Zarubova, Z. Dlabacek, I. Aattio, O. Soderberg, and S. P. Hannula, in *ESOMAT* (2009), p. 04007.
[17]R. W. Overholser, M. Wutting, and D. A. Neumann, Scr. Mater. **40**, 1095 (1999).
[18]Y. Xin, Y. Li, L. Chai, and H. Xu, Scr. Mater. **54**, 1139 (2006).
[19]M. Kreissl, T. Kanomata, M. Matsumoto, K. U. Neumann, B. Ouladdiaf, T. Stephens, and K. R. A. Ziebeck. J. Magn. Magn. Mater. **272**, 2033 (2004).
[20]R. C. O'Handley, J. Appl. Phys. **83**, 3263 (1998).
[21]V. V. Khovailo, T. Takagi, A. N. Vasilev, H. Miki, M. Matsumoto, and R. Kainuma, Phys. Status Solidi A **183**, R1 (2001).
[22]G. K. Williamson and W. H. Hall, Acta Metall. **1**, 22 (1953).
[23]P. Karen and P. M. Woodward, J. Solid State Chem. **141**, 78 (1998).